RESEARCH

Spatiotemporal analysis and seasonality of tuberculosis in Pudong New Area of Shanghai, China, 2014–2023

Shuishui Pan[1†], Lili Chen[1†], Xin Xin[1], Shihong Li[2], Yixing Zhang[1], Yichen Chen[3] and Shaotan Xiao[1*]

Abstract

Background   Spatiotemporal analysis is a vital method that plays an indispensable role in monitoring epidemiological changes in diseases and identifying high-risk clusters. However, there is still a blank space in the spatial and temporal distribution of tuberculosis (TB) incidence rate in Pudong New Area, Shanghai. Consequently, it is crucial to comprehend the spatiotemporal distribution of TB in this district, this will guide the prevention and control of TB in the district.

Methods   Our research used Geographic Information System (GIS) visualization, spatial autocorrelation analysis, and space-time scan analysis to analyze the TB incidence reported in the Pudong New Area of Shanghai from 2014 to 2023, and described the spatiotemporal clustering and seasonal hot spot distribution of TB incidence.

Results   From 2014 to 2023, the incidence of TB in the Pudong New Area decreased, and the mortality was at a low level. The incidence of TB in different towns/streets has declined. The spatial autocorrelation analysis revealed that the incidence of TB was spatially clustered in 2014, 2016–2018, and 2022, with the highest clusters in 2014 and 2022. The high clustering area was mainly concentrated in the northeast. The space-time scan analysis indicated that the most likely cluster was located in 12 towns/streets, with a period of 2014–2018 and a radiation radius of 15.74 km. The heat map showed that there was a correlation between TB incidence and seasonal variations.

Conclusions   From 2014 to 2023, the incidence of TB in the Pudong New Area of Shanghai declined, but there were spatiotemporal clusters and seasonal correlations in the incidence area. Local departments should formulate corresponding intervention measures, especially in high-clustering areas, to achieve accurate prevention and control of TB within the most effective time and scope.

Keywords   Tuberculosis, Spatial autocorrelation analysis, Space-time scan analysis, Seasonality, Pudong New Area

[†]Shuishui Pan and Lili Chen contributed equally to this work as co-first authors.

*Correspondence:
Shaotan Xiao
stxiao@pdcdc.sh.cn
[1]Tuberculosis, AIDS and STD Control Department, Shanghai Pudong New Area Center for Disease Control and Prevention, Shanghai, China
[2]Third Branch Center, Shanghai Pudong New Area Center for Disease Control and Prevention, Shanghai, China
[3]General Management Office , Shanghai Pudong New Area Center for Disease Control and Prevention, Shanghai, China

Background

Tuberculosis (TB) is a disease caused by Mycobacterium TB and transmitted through the respiratory tract. According to statistics, the number of TB infections is statistically high, with approximately a quarter of the global population infected with latent TB in 2014 [1]. Despite being preventable and curable, TB has emerged as the second leading cause of death globally in 2022 [2]. According to the latest report of the World Health Organization, 10.6 million people worldwide were suffering from TB in 2022, with 7.5 million new diagnoses of TB and about 1.3 million deaths [2], which showed that TB remains an important public health problem that jeopardizes public health worldwide [2, 3].TB poses a significant threat to public health in China, as of 2022, China reported 710,000 TB cases, making it the country with the third-highest TB burden globally [2]. Statistics from 2022 indicate that TB-related deaths in China rank second only to those caused by acquired immune deficiency syndrome (AIDS) among notifiable infectious diseases [4]. According to Lin et al. [5], systematic predictions using their model suggest that China may struggle to meet the global goal of ending TB by 2035 with its current prevention and control measures. The TB prevention and control situation in China is quite severe, necessitating further exploration of new strategies and methods. In recent years, spatiotemporal analysis has seen widespread application in clinical hotspot surveillance of infectious diseases. For example, using spatiotemporal analysis for epidemiological monitoring of COVID-19 cases [6], sociodemographic information on zoonotic cutaneous leishmaniasis was clustered based on spatiotemporal analysis [7]. This approach facilitates early detection and active case identification in high-risk areas, guiding the development of relevant prevention and control measures. Moran's spatial autocorrelation analysis and spatial scanning statistics have emerged as widely employed methods to analyze the epidemiological characteristics of TB [8]. A systematic review of the spatial clustering of TB in the global general population revealed that the high-risk attributes of TB correlate with the spatial distribution of hotspots [9]. Identifying the geographical distribution of disease hotspots is helpful for recognizing high-incidence areas and formulating prevention and control measures [10].

Studies conducted in China have demonstrated that the incidence of infectious diseases across different administrative units (provinces, autonomous areas, and municipalities directly under the central government) exhibits temporal and spatial clustering as well as seasonality [11]. The spread and prevalence of TB vary across different cities in China [3]. According to Wei X et al. [12], high-risk areas for TB transmission are primarily located in western and south-central China. However, it is noteworthy that several provinces in eastern China, including Shanghai, are showing a potential upward trend in TB cases. This confirms that the epidemic trend, seasonal patterns, and spatial distribution of TB in different provincial geographical units deserve attention [13]. In addition to spatiotemporal analysis at the provincial and municipal levels [3], the study by Lai P et al. [14]. highlighted the importance of analyzing small-scale TB clusters at the street level. This approach is valuable for determining the prevalence patterns of TB in high-density urban areas. At present, TB prevention and control work in Shanghai is progressing steadily, but special attention should be paid to the prevention and control work in suburban areas [15]. Pudong New Area, the largest district in Shanghai with a permanent population of 5.78 million, warrants a thorough assessment of TB incidence. Understanding the TB situation in Pudong New Area will be essential for effective public health planning and intervention. This study primarily employed spatiotemporal analysis techniques to identify TB clustering areas, investigate the geographical distribution of TB incidence, and uncover gaps in TB prevention and control. The findings will provide a basis for precise TB prevention and control strategies.

Methods

Study area

In this study, the data of Pudong New Area of Shanghai (121°27'l8"E ~ 121°48'43" E, 30°08'20" N ~ 31°23'22" N) were analyzed. It is located in the east of Shanghai, at the mouth of the Yangtze River, and it is the area with the largest population in Shanghai. According to the latest administrative division of Pudong New Area, this study incorporated a total of 36 areas, including 12 streets and 24 towns, as shown in Fig. 1.

Data sources

The TB data for the study was sourced from the Chinese Center for Disease Control and Prevention (CISDCP). This system, developed by the Chinese Center for Disease Control and Prevention, serves medical and health users nationwide. It is the world's largest internet-based disease reporting system, established by the Chinese government after the SARS epidemic in 2003, focusing on the reporting of infectious diseases and public health emergencies [16]. The system utilizes a multi-layer management mechanism to ensure timely and effective data input into CISDCP [17]. After diagnosing cases, hospitals and clinics can directly report infectious diseases via the Internet [16]. Centers for Disease Control can obtain disease information in real time, conduct quality control, and upload the verified data to CISDCP. The number of TB cases was obtained from CISDCP in this study. The demographic data is sourced from the Shanghai Pudong
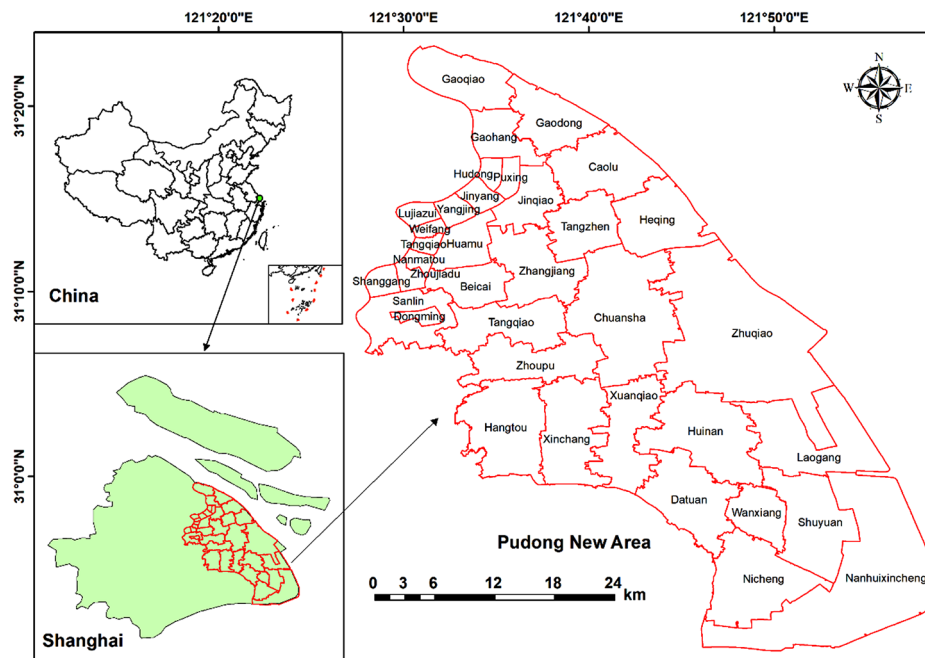
Fig. 1 Geographical location of 36 towns/streets in Pudong New Area of Shanghai

New Area Statistical Yearbook. Considering that the regional division of Pudong New Area in Shanghai has been adjusted many times, to ensure the integrity and availability of demographic data, we extracted all TB case data and demographic data registered and reported in Pudong New Area in Shanghai from January 1, 2014, to December 31, 2023.

Establishment of a spatial information database
At the time of data abstraction, we used Excel tables to organize and construct a database of TB case information, annual total population, and seasonal changes from 2014 to 2023.

Map Digital GIS construction
Geographic Information Systems (GIS) [18] was used to recognize the spatial and temporal patterns of diseases. Taking the administrative planning map of Pudong New Area as the background, the vector maps of 36 towns/streets were established using ArcGIS 10.2 software. Through the coordinate system, GIS was created to implement the visualization of regional TB incidence results. It can be useful in providing readers with explicit and valuable information to comprehend and construe data distributions straightforwardly.

Spatial autocorrelation analysis
Global spatial autocorrelation: This method takes into account all spatial unit data in the entire study, and measures and evaluates the degree of spatial correlation and

difference between them. Moran's I is a spatial autocorrelation metric proposed by Moran [19]. Its calculation formula:

$$I = \frac{n \sum_{i=1}^{n} \sum_{j=1}^{n} w_{ij} \left(x_i - \bar{x}\right) \left(x_j - \bar{x}\right)}{\sum_{i=1}^{n} \sum_{j=1}^{n} w_{ij} (x_i - x)^2} \tag{1}$$

where: n is the number of spatial units indexed by i and j; x is the variable of interest; $\bar{x}$ is the mean of x; w_{ij} are the elements of a matrix of spatial weights with zeroes on the diagonal(i.e., w=0).

Moran's I measures all the metrics that recognize the similarity of observed values of adjacent spatial unit attributes and determines the clustering pattern presented by measuring geographic elements at the global level. The value of I ranges from $-1 \leq I \leq 1$. I>0 indicates a positive spatial correlation. The closer the value is to 1, the higher the degree of spatial clustering. I<0 indicates a negative spatial correlation. I=0 indicates no correlation. We used Z-scores or P-values to recognize whether the indicators were significant. When Moran's I>0 and Z- score≥1.96, $P<0.05$, with statistical significance, the disease shows spatial clustering and statistical clustering.

Local spatial autocorrelation: Global spatial autocorrelation is used to reflect whether the attributes specified in the whole research scope are correlated, but it cannot be pointed out exactly where they are clustered, while local spatial autocorrelation can make up for the above shortcomings. Anselin [20] proposed in 1995 that Local

Moran's I index should be used to measure Local correlation. The formula for calculating Local Moran's I is as follows:

$$I_i = \frac{(x_i - \bar{x})}{\sum_{i=1}^{n}(x_i - \bar{x})^2} \sum_{j=1}^{n} w_{ij}(x_i - \bar{x}) \qquad (2)$$

Where, I_i represents the local Moran's I index of the region, and its relationship with Global Moran's I is

$$I = \sum_{i=1}^{n} \frac{I_i}{n}$$

Using local spatial autocorrelation analysis to identify the correlation between local areas and the distribution of diseases [21, 22]. In the Local indicator of spatial autocorrelation (LISA) plot, using local Moran's I statistics to determine statistical significance, we identified four spatial relational clusters for the analyzed variables, for example, high-high-value clustering areas, low-low-value clustering area, low-high-value clustering areas and high-low-value clustering areas [22]. A positive value I denote that the element has an attribute value that contains the same high or low adjacency factor, which becomes part of the cluster, whereas a negative value I contain the adjacency factor with different values, which is an outlier and not part of the cluster.

Space-time scan analysis

The spatial autocorrelation analysis mentioned above primarily focuses on spatial clustering without incorporating

the time factor, thus hindering the determination of temporal trends in geospatial clustering areas. To address this limitation, SaTScan software developed by Kulldorff [23] offers an effective solution. The statistical method of space-time scan analysis considers both space and time, and the statistical method of spatiotemporal scanning analysis considers both space and time simultaneously. Space-time scan analysis is a clustering method based on a dynamic cylindrical window that has a circular geographic graphic basis, the window moves in space and space, and the height corresponds to time. The incidence of TB is assumed to follow the Poisson distribution, and the Poisson probability model is used to construct the log-likelihood ratio (LLR) under this assumption. Statistical tests are then performed using the Monte Carlo simulation method and p-values are calculated. Large LLR values and statistically significant differences indicate that the region contained under this dynamic window has a higher probability of aggregation [24, 25].

Statistical analysis

We utilized GIS 10.2 to illustrate the spatial pattern of annual TB incidence across 36 towns/streets in Pudong New Area from 2014 to 2023. To determine the presence of spatial autocorrelation at the regional level, we conducted an analysis using Geoda 1.22.0.4 software. Additionally, we performed space-time scan analysis with SatScan 10.1.3 software to depict the spatiotemporal distribution of TB incidence.

Results

Epidemiological characteristics

A total of 14,104 cases of TB were reported in the Pudong New Area of Shanghai from January 2014 to December 2023. The characteristics of 14,104 TB cases are shown in Table 1. The male-to-female ratio was 1.99:1, with 9394 males and 4710 females. The age group of >60 accounted for the largest proportion (35.05%), and the main affected group was retirees (26.71%).

From 2014 to 2022, with an average annual incidence of 25.14 cases per 100,000 persons, the incidence of TB showed a downward trend, with the most significant decline in 2022. The annual incidence of TB in 2023 has increased slightly, but it was still lower than the incidence of TB in 2021 and before. As shown in Fig. 2.

In the study area comprising 36 towns/streets, the reported annual incidence of TB has exhibited a decreasing trend from 2014 to 2023 across various towns/streets, as illustrated in Fig. 3.

Utilizing the annual incidence of the district as the baseline (25.14 cases per 100,000), a comparison was made between the light blue and light red dividing lines, as depicted in Fig. 4. The impact of the novel coronavirus epidemic in 2022 resulted in reported TB incidences in

Table 1 Demographic characteristics of patients with TB in Pudong New Area, Shanghai, 2014–2023

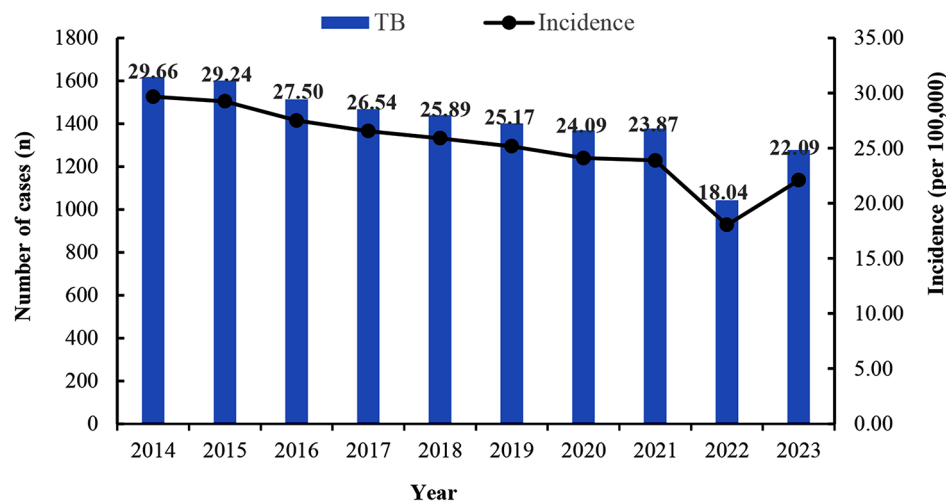| Variables	Case number	Percentage (%)
Gender		
Female	4710	33.39
Male	9394	66.61
Age		
0–15 year	24	0.17
16-30year	2241	15.89
31-45year	4557	32.31
46-60year	2338	16.58
>60 year	4944	35.05
Occupation		
Retiree	3768	26.71
Housework and unemployment	3131	22.20
Peasant	1348	9.56
Commercial service	712	5.05
Student	599	4.25
Worker	367	2.60
Others	2764	19.60
Unknown	1415	10.03

Fig. 2 Overall TB prevalence in Pudong New Area, Shanghai, 2014-202. *Distribution of TB in 36 towns/streets*

each area falling below the baseline. Furthermore, over time, there has been a decline in the number of towns/streets where TB incidences surpass the baseline, evident by the gradual transition from the red area to the blue area in Fig. 4. In the longitudinal comparison across different years within the same street, it is observed that the reported incidence of TB in Laogang Town has consistently remained lower than the baseline over the past decade. Conversely, the reported TB incidences in Hudongxincun Street and Tangqiao Street have been higher than the baseline for nine consecutive years.

Spatial autocorrelation analysis

Global spatial autocorrelation analysis of the annual incidence of TB in the study in the Pudong New Area from 2014 to 2023 showed that Moran's I was significant (Table 2). Among them, the incidence of TB from 2014, 2016 to 2018, and 2022 showed a positive spatial clustering correlation (Moran's I value > 0, and z value > 1.96, and P value < 0.05), of which 2014 (Moran's I value = 0.457) and 2022 (Moran's I value = 0.384) had the highest positive spatial correlation, as shown in Table 2.

From 2014 to 2023, local spatial autocorrelation analysis of the annual incidence of TB in the Pudong New Area revealed the presence of high-high-value clustering areas (hot spots) and low-low-value clustering areas (cold spots). We conducted a summary and analysis of these "hot spot" and "cold spot" clustering areas at a test level of 0.05, identifying the highest statistically significant clustering areas in 2022 (a total of 12 clustering areas), followed by 2014 (11 clustering areas), 2018 (11 clustering areas), and 2019 (11 clustering areas). According to the survey, there have been slight changes in the TB hotspots in the area each year. From 2014 to 2023, TB hotspots were consistently identified in Caolu Town,

Gaoqiao Town, Gaohang Town, Gaodong Town, Jinqiao Town, and Hudong Xincun Street in the northeast of the district, with Caolu Town emerging as a hotspot for five years, as shown in Fig. 5.

Space-time scan analysis

From 2014 to 2023, there exists one most likely cluster spatiotemporal clustering area and one secondary spatiotemporal clustering area. The first-level spatiotemporal clustering area was located in 12 towns/streets, including Cao Lu, Gaodong, Gaohang, Hudong, etc., with a period from 2014 to 2018. As the most likely cluster, the first-level spatiotemporal clustering area contained 3,125 cases, with an expected number of 2,457 cases, and a radiation radius of 15.74 km (log-likelihood ratio LLR = 102.78, relative risk RR = 1.35), with a difference of $P < 0.001$, which was statistically significant, as shown in Fig. 6.

Heat map of seasonal distribution of TB incidence

This area exhibits a seasonal correlation. Except for the epidemic years (2020–2022), late spring (March) marks the high period of TB incidence, while February sees lower incidences. The seasonal peak period varies from year to year, with summer (April-June) and autumn (July-September) being the clustered peak periods for TB incidence. This seasonal pattern is most prominent from 2014 to 2021, as illustrated in Fig. 7.

Discussion

To the best of our knowledge, this study represented the first attempt to elucidate the trends in TB incidence and its spatial patterns in the Pudong New Area. There were 14,104 TB patients in the region in the past decade, the ratio of male to female patients was 1.99, slightly higher
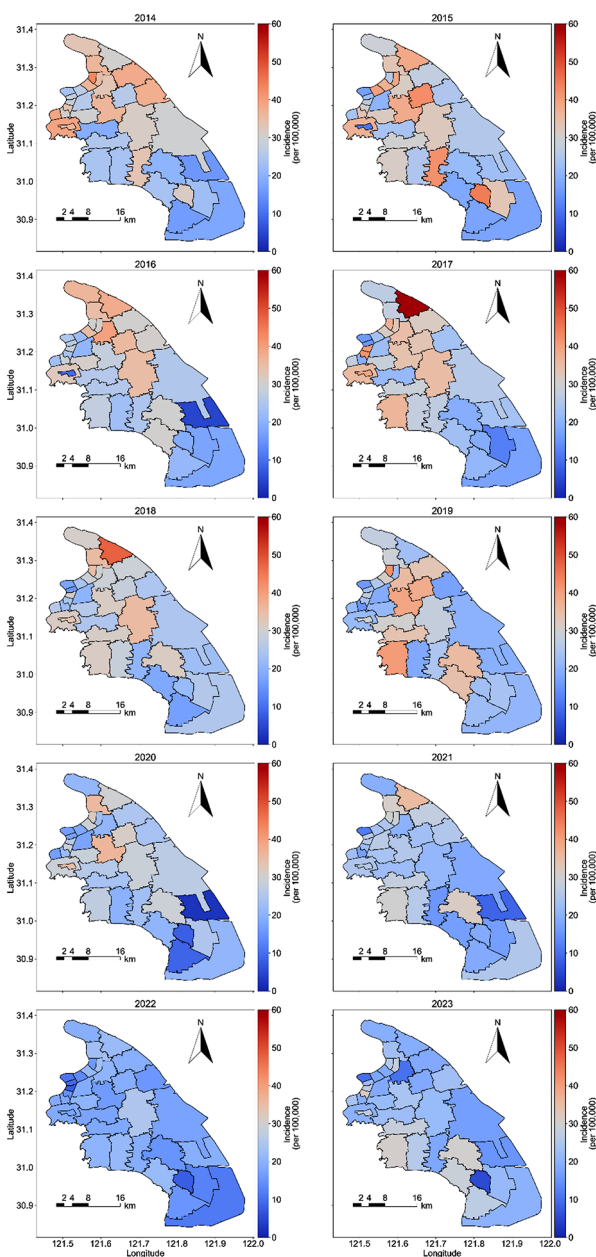
Fig. 3 Overall distribution of TB in 36 towns/streets, 2014–2023

Fig. 4 Comparison of TB baseline in 36 towns/streets, 2014–2023

than in another study in China (1.83) [26]. In addition, the number of elderly TB patients > 60 years old in this area is the largest, which is consistent with the study of Li SJ, et al. [27]. It is worth noting that the proportion of retired TB patients in this area is the highest, which indicates that we need to strengthen the prevention and control of TB in the elderly.

Over the past decade, the incidence of TB in this area has exhibited a decreasing trend, consistent with national and some provincial studies [12, 25, 28]. This can be largely attributed to the effective guidance of TB prevention and control management in China, coupled
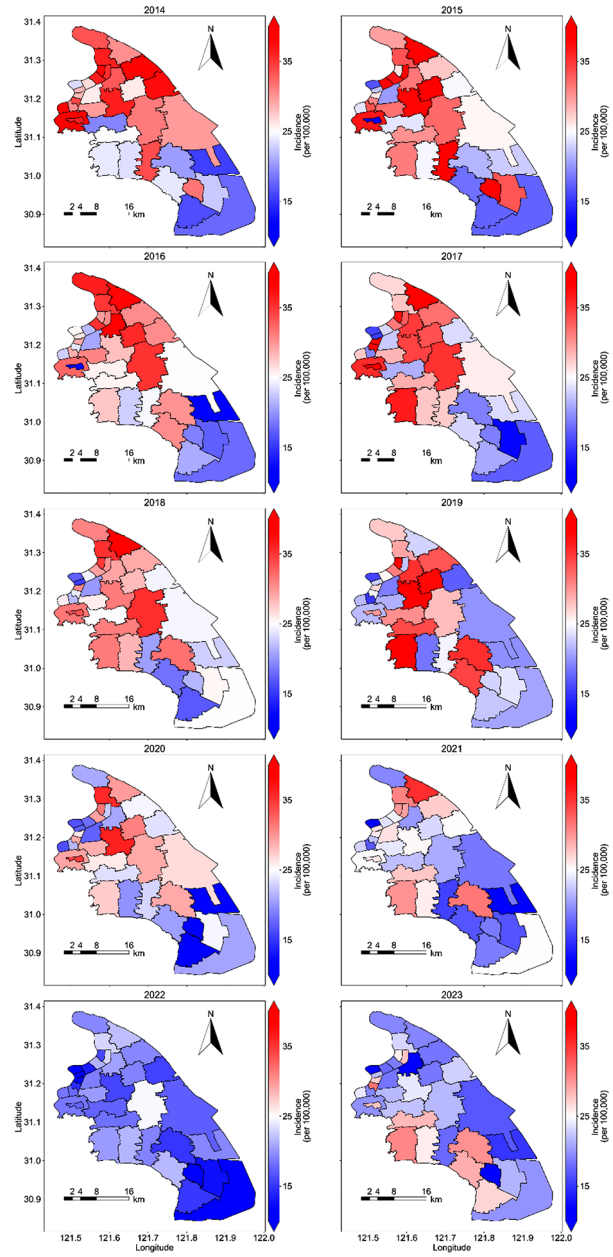
with the high attention paid to TB prevention and control by municipal governments and health administration departments [29]. In recent years, relevant municipal departments in Shanghai have diligently executed the objectives outlined in the "13th Five-Year Plan for TB Prevention and Control in Shanghai." These efforts include enhancing the capacity and awareness of TB prevention and control, increasing investment in research funds, and effectively managing the diagnosis, treatment, and care of TB patients [30].

It was pertinent to highlight the observed differences in TB incidence among the towns/streets. Throughout

Table 2 Results of Moran's *I* analysis of the annual incidence cases of TB, 2014–2023

Year	*Moran's I* value	Z value	P value	Pattern
2014	0.457	4.344	0.000	Clustered
2015	-0.145	-1.045	0.296	Dispersed
2016	0.299	2.933	0.003	Clustered
2017	0.259	2.567	0.010	Clustered
2018	0.372	3.586	0.000	Clustered
2019	0.125	1.372	0.170	Dispersed
2020	0.163	1.718	0.086	Dispersed
2021	0.086	1.024	0.306	Dispersed
2022	0.384	3.701	0.000	Clustered
2023	-0.029	-0.008	0.994	Dispersed

the study period, there has been a downward trend in the number of towns/streets with reported TB incidence exceeding the baseline. Upon longitudinal comparison across years within each area, it was found that only Lao-gang Town consistently exhibited low TB incidence over ten years. Conversely, Hudong Xincun Street and Tangqiao Street reported higher than baseline TB incidence for nine consecutive years, potentially influenced by local population density. It is worth noting that the population density of the latter two areas is three times that of

the former. Elevated population density tends to facilitate germ transmission. Moreover, internal migration mobility [31] could emerge as a significant factor influencing TB incidence, given the observed correlation between migration and TB incidence.

Spatial autocorrelation analysis has revealed that the spatial distribution of TB incidence was not random. The high clustering observed in 2014 has not found similar results in relevant studies. We think it may be that the TB prevention and control measures were not perfect in the early years compared with the present, and 2014 is the first year of our research, so we will observe that the clustering is higher than that in other years. Conversely, the heightened concentration in 2022 can be explained by the severe impact of the novel coronavirus epidemic in Shanghai during that year, resulting in delays in diagnosis and treatment for potential TB cases. Moreover, localized transmission of the novel coronavirus, alongside the invasion of TB, heightened the susceptibility of the population to TB infection, thereby increasing the risk of TB clustering. However, it's noteworthy that low staff turnover during this period likely mitigated the spread of TB on a larger scale. This phenomenon serves as a compelling confirmation that 2022 represented a
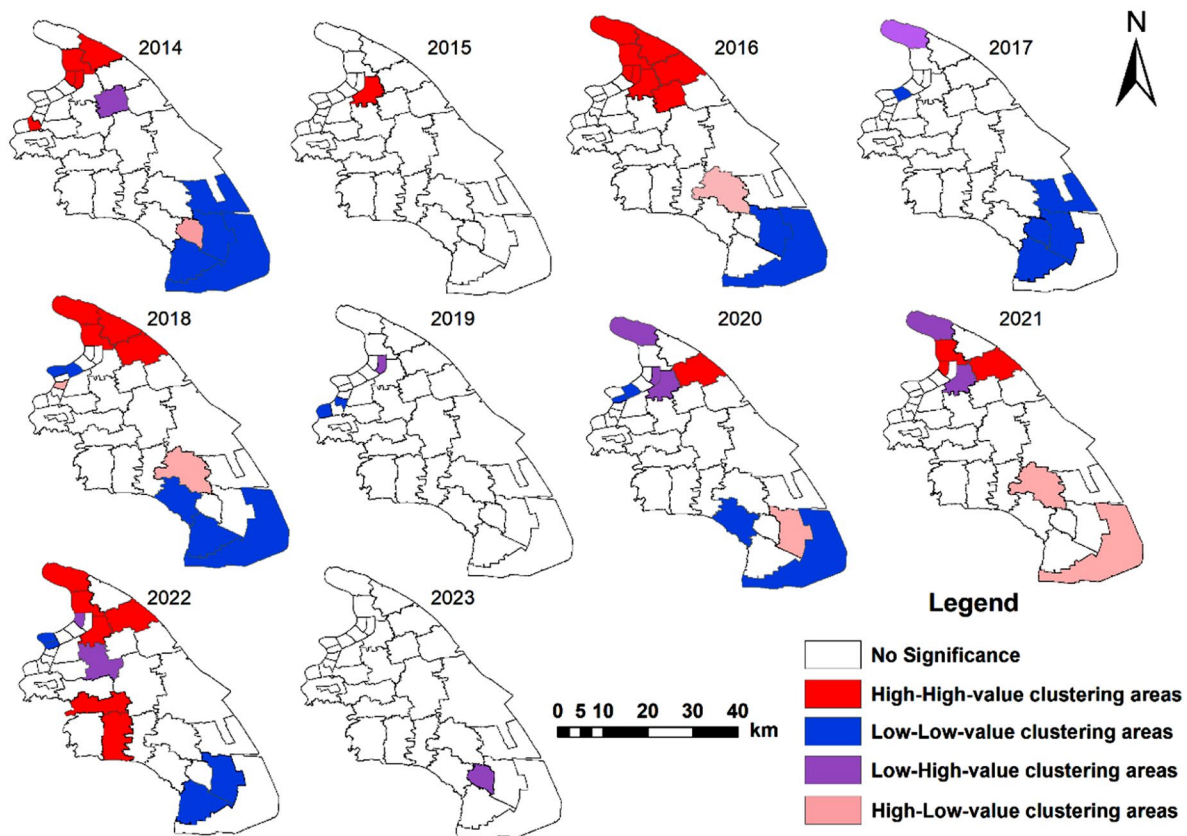
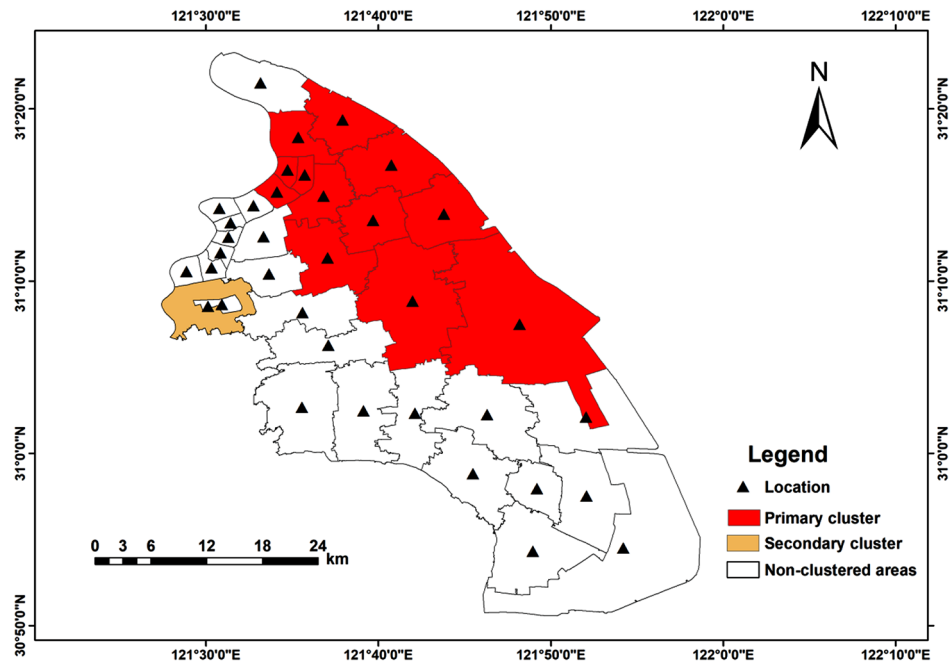**Fig. 5** Local spatial autocorrelation analysis of TB in 36 towns/streets, 2014–2023

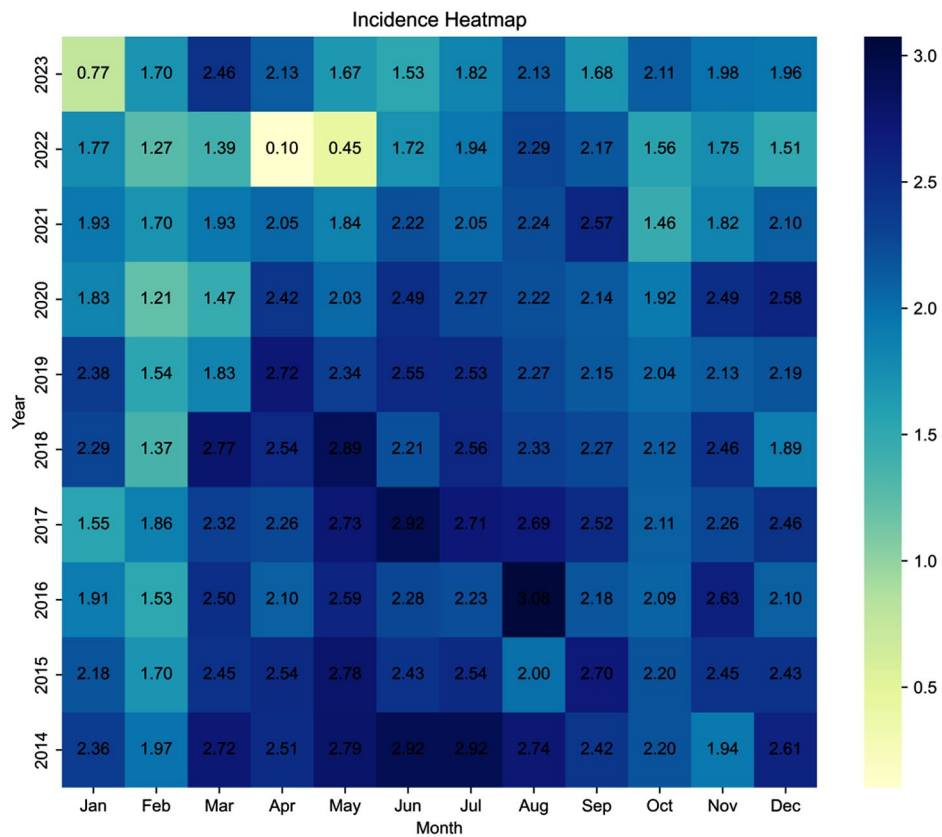**Fig. 6** Spatiotemporal clustering analysis of TB incidence, 2014–2023

Fig. 7 Heat maps of seasonal distribution of TB in 36 towns/streets

high-concentration area of TB, despite the overall low annual incidence.

Further local spatial analysis revealed a growing trend in the number of clusters of TB incidence as time progressed, this finding aligned with the results of Guo C [32] in their study on TB in mainland China. Our study highlighted that high TB incidence was primarily concentrated in the northeast of the district, especially, Caolu Town emerged as a hot spot for five years. These trends may be attributed to local population dynamics, economic development, and healthcare infrastructure. The study underscored the importance of strengthening TB-related health education, conducting regular job training, and enhancing the management system for TB. Additionally, variations in TB incidence among different towns/streets and over time suggest that TB prevention and control efforts have not yet reached a stable level. Therefore, each area must consider past trends in the TB epidemic when formulating prevention and control strategies for the upcoming years, ensuring strict adherence to overall prevention and control measures.

In our study, one primary cluster and one secondary cluster indicate divergent time trends in TB prevalence across different towns/streets. The primary spatiotemporal clustering area was observed during 2014–2018, suggesting that the burden of TB incidence decreased after 2018. This decline could be attributed to heightened attention from national and local authorities towards TB prevention and control measures [30]. Notably, the issuance of the "National Tuberculosis Prevention and Control Plan (2011–2015)" by the General Office of the State Council in November 2011 marked a pivotal step, outlining a series of strategies for TB prevention and control [33]. Subsequently, during the implementation of the "Thirteenth Five-Year Plan" (2016–2020), Shanghai continued to enhance its TB prevention and control service system in alignment with these guidelines, further bolstering the effective management of TB [30]. The results of space-time analysis revealed that TB clustering primarily occurred in the northeast of the district. Factors influencing TB clustering areas include population mobility, lifestyle choices, environmental factors, and socioeconomic disparities. In high-concentration areas, the health system, led by the CDC and in collaboration with community health service centers, should carry out targeted health interventions based on community diagnosis results. The northeastern part of the region, characterized by a mix of urban and rural areas and a large population flow, requires focused TB health education and active screening of key and high-risk groups. These efforts aim to maximize the early detection of patients and latent infections.

Further exploration was conducted into the seasonal hot spots of TB distribution. Regarding the reporting of seasonal TB incidence, excluding the three-year epidemic period (2020–2022), the end of spring (March) emerged as the peak clustering period for TB reports. This finding aligns with national TB surveillance results [34]. The high incidence of TB reported in March can be attributed to delays in consultation and diagnosis of TB patients [35]. This delay likely results in a backlog of cases being reported in March. The formation of peaks in March may be linked to the window period of increased susceptibility to TB, which typically commences in winter. Patients infected with TB may exhibit symptoms and seek medical treatment within 2–3 months. Notably, there is a correlation between vitamin D deficiency and the development of TB [36]. Vitamin D deficiency is more common in TB patients than in the normal population [37]. Normal vitamin D metabolism activates macrophages, effectively inhibiting the intracellular production of TB. Low synthesis of vitamin D in winter poses a risk of latent TB infection for susceptible individuals [38].

Our study also found that the peak stage of the disease was different each year, and the specific reasons remain to be explored, but these may be mixed with non-seasonal factors because Wang H, et al. [39] found that there was a correlation between the seasonal appearance of environmental air pollutants and TB. The high-incidence seasons reported in our study are summer (April-June) and autumn (July-September). Our findings coincide with the seasonality of TB reporting observed in various areas, including Hubei (late spring/early summer) [28], Guangxi (spring and summer) [40], Germany (late spring/late summer) [41], Japan (summer-fall) [42], Pakistan (April-June) [43], and New York (March-May) [44]. These variations in reporting periods may be attributed to differences in geographical areas among the subjects included in various studies, as well as the influence of local climate and environmental factors on TB spread [45]. Furthermore, the increased latent disease activity during winter and early spring may contribute to a surge in patient visits and subsequent seasonal reporting in the following months. In summary, the observed seasonal peak in reported TB incidence underscores the temporal concentration of cases. Therefore, intensifying efforts in TB prevention and control during winter and spring, and enhancing awareness of protective measures, will aid in mitigating the issue of seasonal TB incidence.

Our study has several limitations that should be acknowledged. Firstly, the analysis conducted focused solely on spatiotemporal patterns of TB incidence. Regional-scale effects may introduce errors in the results, potentially masking correlations with factors such as regional economy, population education level, and healthcare infrastructure. Secondly, while our study identified seasonal patterns in TB incidence, we did not obtain relevant data to explore the influence of local

Pan *et al. BMC Infectious Diseases*   (2024) 24:761

Page 10 of 11

temperature and environmental factors on seasonal TB incidence. This represents a gap in our analysis and warrants further investigation in future research. Lastly, the data for our study were obtained from the self-monitoring system, and there may have been missing information on TB patients, leading to potential data bias in our analysis. Acknowledging these limitations is crucial for interpreting the findings of our study accurately and for guiding future research efforts to address these gaps.

Conclusions

In our study, spatiotemporal analysis has demonstrated its reliability in epidemiological research. Over the period from 2014 to 2023, the reported incidence of TB in the Pudong New Area of Shanghai exhibited a declining trend. Our study has identified spatiotemporal clustering as well as seasonal correlations in TB incidence. High clustering areas were primarily concentrated in the northeastern part of the district, with March identified as the period of peak TB incidence. Relevant departments should make effective use of information from high-risk areas and selectively expand the scope of health prevention and control, especially in areas with high incidences of TB, which will be the next key work in the Pudong New Area.

Abbreviations
TB   Tuberculosis
GIS   Geographic Information System
CISDCP   Chinese Center for Disease Control and Prevention
LISA   Local indicator of spatial autocorrelation
Moran's I   Moran's index
LLR   Log-likelihood ratio

Declarations

Ethics approval and consent to participate
The studies involving human participants were reviewed and approved by the Ethics Committee of the Pudong New Area Center for Disease Control and Prevention. The Centre for Disease Control and Prevention of Shanghai Pudong New Area, which is information from the China Epidemiological Information Network, has strict confidentiality. Written informed consent for participation was not required for this study by the national legislation and the institutional requirements.

Consent for publication
Not applicable.

Competing interests
The authors declare no competing interests.

References
1. Houben RMGJ, Dodd PJ. The global burden of latent tuberculosis infection: a re-estimation using mathematical modelling. PLoS Med. 2016;13(10):e1002152. https://doi.org/10.1371/journal.pmed.1002152.
2. World Health Organization.Global pulmonary tuberculosis report 2022 [Internet]. 2023. https://www.who.int/publications/i/item/9789240083851. Accessed 7 Feb 2024.
3. Bai W, Ameyaw EK. Global, regional and national trends in tuberculosis incidence and main risk factors: a study using data from 2000 to 2021. BMC Public Health. 2024;24(1):12. https://doi.org/10.1186/s12889-023-17495-6.
4. National Health Commission. Statistical Bulletin of China's Health Development in 2022 [Internet]. In 2022. http://www.nhc.gov.cn/guihuaxxs/s3585u/202309/6707c48f2a2b420fbfb739c393fcca92.shtml Accessed 19 June 2024.
5. Lin HH, Wang L, Zhang H, Ruan Y, Chin DP, Dye C. Tuberculosis control in China: use of modelling to develop targets and policies. Bull World Health Organ. 2015;93(11):790–8. https://doi.org/10.2471/BLT.15.154492.
6. Tabasi M, Alesheikh AA, Babaie E, Hatamiafkoueieh J. Spatiotemporal surveillance of COVID-19 based on epidemiological features: evidence from Northeast Iran. Sustainability. 2022;14(19):12189. https://doi.org/10.3390/su141912189.
7. Tabasi M, Alesheikh AA. Spatiotemporal variability of zoonotic cutaneous leishmaniasis based on Sociodemographic Heterogeneity. The case of northeastern Iran, 2011–2016. Jpn J Infect Dis. 2021;74(1):7–16. https://doi.org/10.7883/yoken.JJID.2020.048.
8. Shaweno D, Karmakar M, Alene KA, Ragonnet R, Clements AC, Trauer JM, et al. Methods used in the spatial analysis of tuberculosis epidemiology: a systematic review. BMC Med. 2018;16(1):193. https://doi.org/10.1186/s12916-018-1178-4.
9. Teibo TKA, Andrade RLP, Rosa RJ, Tavares RBV, Berra TZ, Arcêncio RA. Geospatial high-risk clusters of tuberculosis in the global general population: a systematic review. BMC Public Health. 2023;23(1):1586. https://doi.org/10.1186/s12889-023-16493-y.
10. Bekele D, Aragie S, Alene KA, Dejene T, Warkaye S, Mezemir M, et al. Spatiotemporal distribution of tuberculosis in the Oromia Region of Ethiopia: a Hotspot Analysis. Trop Med Infect Dis. 2023;8(9):437. https://doi.org/10.3390/tropicalmed8090437.
11. Zheng J, Zhang N, Shen G, Liang F, Zhao Y, He X, et al. Spatiotemporal and seasonal trends of Class A and B Notifiable Infectious diseases in China: retrospective analysis. JMIR Public Health Surveill. 2023;9:e42820. https://doi.org/10.2196/42820.
12. Wei X, Fu T, Chen D, Gong W, Zhang S, Long Y, et al. Spatial-temporal patterns and influencing factors for pulmonary tuberculosis transmission in China: an analysis based on 15 years of surveillance data. Environ Sci Pollut Res Int. 2023;30(43):96647–59. https://doi.org/10.1007/s11356-023-29248-4.
13. Mao Y, He R, Zhu B, Liu J, Zhang N. Notifiable respiratory infectious diseases in China: a spatial-temporal epidemiology analysis. Int J Environ Res Public Health. 2020;17(7):2301. https://doi.org/10.3390/ijerph17072301.
14. Lai P, Cai W, Qu L, Hong C, Lin K, Tan W, Zhao Z. Pulmonary tuberculosis notification rate within Shenzhen, China, 2010–2019: spatial-temporal analysis. JMIR Public Health Surveill. 2024;10:e57209. https://doi.org/10.2196/57209.
15. Wang YT, Peng WJ, Su HL, Rao LX, Wang WB, Shen X. [Spatial-temporal characteristics and influencing factors of pulmonary tuberculosis cases in Shanghai from 2013 to 2020]. Zhonghua Liu Xing Bing Xue Za Zhi. 2023;44(8):1231–6. https://doi.org/10.3760/cma.j.cn112338-20221128-01006. Chinese.

16. Wang L, Wang Y, Jin S, Wu Z, Chin DP, Koplan JP, Wilson ME. Emergence and control of infectious diseases in China. Lancet. 2008;372(9649):1598–605. https://doi.org/10.1016/s0140-6736(08)61365-3.

17. Zhang L, Wilson DP. Trends in notifiable infectious diseases in China: implications for surveillance and population health policy. PLoS ONE. 2012;7(2):e31076. https://doi.org/10.1371/journal.pone.0031076.

18. Bailey TC. Spatial statistical methods in health. Cad Saude Publica. 2001;17(5):1083–98. https://doi.org/10.1590/s0102-311x2001000500011.

19. Moran PA. Notes on continuous stochastic phenomena. Biometrika. 1950;37(1–2):17–23.

20. Anselin L. Local indicators of spatial association-LISA. Geograph Anal. 1995;27(2):93–115. https://doi.org/10.1111/j.1538-4632.1995.tb00338.x.

21. Vilinová K. Spatial autocorrelation of breast and prostate cancer in Slovakia. Int J Environ Res Public Health. 2020;17:4440. https://doi.org/10.3390/ijerph17124440.

22. Moraga P, Montes F. Detection of spatial disease clusters with LISA functions. Stat Med. 2011;30(10):1057–71. https://doi.org/10.1002/sim.4160.

23. Kulldorff M. A spatial scan statistic. Commun Stat. 1997;26(6):1481–96.

24. Kulldorff M, Athas WF, Feurer EJ, Miller BA, Key CR. Evaluating cluster alarms: a space-time scan statistic and brain cancer in Los Alamos, New Mexico. Am J Public Health. 1998;88(9):1377–80.

25. Yu Y, Wu B, Wu C, Wang Q, Hu D, Chen W. Spatial-temporal analysis of tuberculosis in Chongqing, China 2011–2018. BMC Infect Dis. 2020;20(1):531. https://doi.org/10.1186/s12879-020-05249-3.

26. Kang W, Yu J, Liang C, Wang Q, Li L, Du J, et al. Epidemiology and Association Rules Analysis for pulmonary tuberculosis cases with Extrapulmonary tuberculosis from age and gender perspective: a large-scale Retrospective Multicenter Observational Study in China. Int J Clin Pract. 2023;2023:5562495. https://doi.org/10.1155/2023/5562495.

27. Li SJ, Li YF, Song WM, Zhang QY, Liu SQ, Xu TT, An QQ, Liu JY, Li HC. Population aging and trends of pulmonary tuberculosis incidence in the elderly. BMC Infect Dis. 2021;21(1):302. https://doi.org/10.1186/s12879-021-05994-z.

28. Zhang Y, Ye J, Hou S, Lu X, Yang C, Pi Q, et al. Spatial-temporal analysis of pulmonary tuberculosis in Hubei Province, China, 2011–2021. PLoS ONE. 2023;18(2):e0281479. https://doi.org/10.1371/journal.pone.0281479.

29. China Center for Disease Control and Prevention. Technical Guidelines for Tuberculosis Prevention and Control in China [Internet]. 2023. https://tb.chinacdc.cn/xxjlg/202111/W020211119672904030470.pdf Accessed 31 May 2024.

30. General Office of Shanghai Municipal People's Government. Notice of the General Office of the Shanghai Municipal People's Government on the issuance of the 13th Five-Year Plan for tuberculosis prevention and treatment in Shanghai [Internet].2017. https://www.shanghai.gov.cn/nw12344/20200814/0001-12344_54245.html Accessed 7 Feb 2024.

31. He WC, Ju K, Gao YM, Zhang P, Zhang YX, Jiang Y, et al. Spatial inequality, characteristics of internal migration, and pulmonary tuberculosis in China, 2011–2017: a spatial analysis. Infect Dis Poverty. 2020;9(1):159. https://doi.org/10.1186/s40249-020-00778-0.

32. Guo C, Du Y, Shen SQ, Lao XQ, Qian J, Ou CQ. Spatiotemporal analysis of tuberculosis incidence and its associated factors in mainland China. Epidemiol Infect. 2017;145(12):2510–9. https://doi.org/10.1017/S0950268817001133.

33. General Office of the State Council. Notice of the Office of the State Council on the Issuance of the National Tuberculosis Prevention and Control Plan (2011–2015) [Internet]. 2011. https://www.gov.cn/gongbao/content/2011/content_2020914.htm Accessed 27 Feb 2024.

34. Zuo Z, Wang M, Cui H, Wang Y, Wu J, Qi J, et al. Spatiotemporal characteristics and the epidemiology of tuberculosis in China from 2004 to 2017 by the nationwide surveillance system. BMC Public Health. 2020;20(1):1284. https://doi.org/10.1186/s12889-020-09331-y.

35. Batbayar B, Kariya T, Boldoo T, Purevdorj E, Dambaa N, Saw YM, et al. Patient delay and health system delay of patients with newly diagnosed pulmonary tuberculosis in Mongolia, 2016–2017. Nagoya J Med Sci. 2022;84(2):339–51. https://doi.org/10.18999/nagjms.84.2.339.

36. Hsu MS, Chung TC, Wang PH, Cheng SL, Wu YW, Hsu JC, et al. Revisiting the association between vitamin D deficiency and active tuberculosis: a prospective case-control study in Taiwan. J Microbiol Immunol Infect. 2024;57(3):490–7. https://doi.org/10.1016/j.jmii.2024.03.005.

37. Mamadapur VK, Nagaraju S, Prabhu MM. Comparative Study of Vitamin D Levels in newly diagnosed tuberculosis and a normal Population. Med (Kaunas). 2024;60(5):685. https://doi.org/10.3390/medicina60050685.

38. Willis MD, Winston CA, Heilig CM, Cain KP, Walter ND, Mac Kenzie WR. Seasonality of tuberculosis in the United States, 1993–2008. Clin Infect Dis. 2012;54(11):1553–60. https://doi.org/10.1093/cid/cis235.

39. Wang H, Tian C, Wang W, Luo X. Temporal cross-correlations between ambient air pollutants and seasonality of tuberculosis: a time-series analysis. Int J Environ Res Public Health. 2019;16(9). https://doi.org/10.3390/ijerph16091585.

40. Cui Z, Lin D, Chongsuvivatwong V, Zhao J, Lin M, Ou J, et al. Spatiotemporal patterns and ecological factors of tuberculosis notification: a spatial panel data analysis in Guangxi, China. PLoS ONE. 2019;14(5):e0212051. https://doi.org/10.1371/journal.pone.0212051.

41. Charles T, Eckardt M, Karo B, Haas W, Kröger S. Seasonality in extra-pulmonary tuberculosis notifications in Germany 2004-2014- a time series analysis. BMC Public Health. 2021;21(1):661. https://doi.org/10.1186/s12889-021-10655-6.

42. Manabe T, Takasaki J, Kudo K. Seasonality of newly notified pulmonary tuberculosis in Japan, 2007–2015. BMC Infect Dis. 2019;19(1):497. https://doi.org/10.1186/s12879-019-3957-8.

43. Butt MF, Younis S, Wu Z, Hadi SH, Latif A, Martineau AR. The relationship between seasonality, latitude and tuberculosis notifications in Pakistan. BMC Infect Dis. 2021;21(1):210. https://doi.org/10.1186/s12879-021-05899-x.

44. Parrinello CM, Crossa A, Harris TG. Seasonality of tuberculosis in New York City, 1990–2007. Int J Tuberc Lung Dis. 2012;16(1):32–7. https://doi.org/10.5588/ijtld.11.0145.

45. Li H, Ge M, Zhang M. Spatio-temporal distribution of tuberculosis and the effects of environmental factors in China. BMC Infect Dis. 2022;22(1):565. https://doi.org/10.1186/s12879-022-07539-4.

Publisher's Note